Femtosecond shaping of transverse and longitudinal light polarization

Tobias Brixner and Walter Pfeiffer

Physikalisches Institut, Universität Würzburg, Am Hubland, 97074 Würzburg, Germany

F. Javier García de Abajo

Centro Mixto Consejo Superior de Investigaciones Científicas/Universidad del País Vasco, Apartado 1072, 20080 San Sebastián, Spain

Received March 29, 2004

Femtosecond laser pulse shaping techniques have been restricted to propagating transverse electromagnetic waves. We present a scheme for pulse shaping of optical near fields based on the excitation of longitudinal electromagnetic fields with polarization-shaped light pulses. By solving Maxwell's equations for a model nanostructure, i.e., a scanning tunneling microscope tip, with help from the boundary-element method, we demonstrate that the electric field vector oscillates in a complex yet controllable fashion in three dimensions. Many applications are envisioned because literally another dimension in the optimal control of light–matter interaction is accessible. © 2004 Optical Society of America

OCIS codes: 320.5540, 260.5430.

Femtosecond laser pulse shaping[1] has led to experimental breakthroughs in many areas, such as quantum control.[2,3] LCDs can be used to modulate the phase[4] or phase and amplitude[5] of individual frequency components, and with two-dimensional LCDs even spatiotemporal properties can be controlled.[6] However, in all cases the polarization state of the shaped light pulse remains linear. With polarization pulse shaping[7–9] two transverse electric field components of femtosecond laser pulses can be phase shaped independently. Thereby it is possible to vary the polarization state of light (i.e., ellipticity and angle of orientation) as well as the intensity and momentary frequency as functions of time within a single laser pulse, which has been applied, e.g., in optimized anti-Stokes Raman spectroscopy.[10]

Here we show how in addition to transverse polarizations the longitudinal component of light fields can be controlled on a femtosecond time scale, thus opening the door to the third and last dimension in the manipulation of electric field profiles and light–matter interaction. This three-dimensional (3D) control of the electromagnetic field is achieved in the vicinity of a suitable nanostructure that is illuminated by polarization-shaped laser pulses. We demonstrate this rather general scheme for a model geometry, i.e., a scanning tunneling microscope tip that is positioned above a nanoscale sphere (Fig. 1). Femtosecond laser pulses are modified in a femtosecond pulse shaper.[7,8] A two-layer LCD in the Fourier plane of a $4f$ configuration compressor introduces phase retardations $\Phi^{(1)}(\omega)$ and $\Phi^{(2)}(\omega)$ for two mutually orthogonal (transverse) polarization directions. The resulting pulses are irradiated onto the chosen nanostructure. In the vicinity of the tip strong local field enhancement can be observed.[11] Furthermore, the electric field acquires a longitudinal component that, like the transverse components, depends on the external pulse structure.

A correct theoretical treatment requires us to take into account the time-dependent vectorial characteristics of the electric field, the given geometry, material dispersion properties, and electromagnetic propagation and retardation effects. We solve the frequency-dependent Maxwell equations by means of the boundary-element method.[12,13] This is a Green's function approach, in which equivalent surface charges and currents are introduced to account for both external sources and induced sources beyond boundary surfaces. A self-consistent solution is then obtained under the constraint that the usual electromagnetic boundary conditions are satisfied. This leads to surface-integral equations that can be further simplified by making use of the axial symmetry and

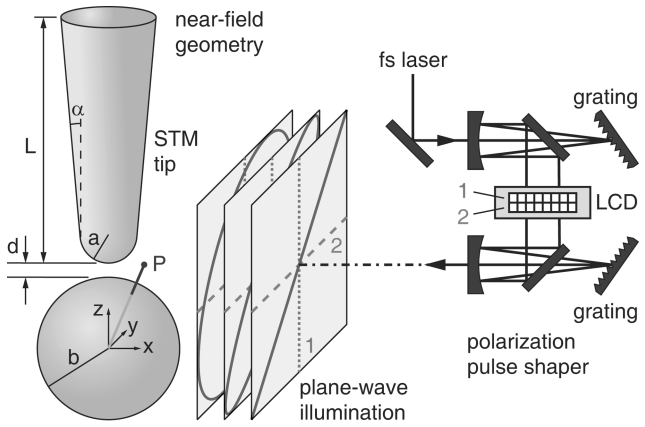

Fig. 1. Proposed experimental arrangement. A femtosecond polarization pulse shaper (right side) manipulates the spectral phases of two polarization components 1 and 2 in 128 independent frequency intervals (from 670 to 890 nm). These laser pulses with time-varying but transverse polarization states are irradiated as a plane wave onto the near-field geometry (left side, material: gold) with sample radius $b = 25$ nm, tip radius $a = 10$ nm, cone half-angle $\alpha = 5°$, length $L = 1500$ nm, and tip–sample separation $d = 5$ nm. The local electric field thus acquires two transverse and one longitudinal polarization components and is calculated at any point $P(\mathbf{r})$ by solving Maxwell's equations with help from the boundary-element method. STM, scanning tunneling microscope.

0146-9592/04/182187-03$15.00/0

Fourier decomposition. The method is easily adapted for any axially symmetric configuration. Other geometries can be calculated as well in principle but without the additional speed advantage of Fourier decomposition. This calculation is performed twice, assuming purely 1-polarized and 2-polarized input fields, respectively. As a result, we obtain complex-valued matrices $A_\alpha{}^{(i)}(\mathbf{r},\omega)$, where the subscripts $\alpha = x, y, z$ indicate the component of the electric field at point $\mathbf{r}$ and frequency ω induced by a far field of superscripted linear polarization $i = 1$ or $i = 2$. The amplitudes in $A_\alpha{}^{(i)}(\mathbf{r},\omega)$ describe the extent to which the two far-field components 1 and 2 couple to the local field, whereas the phases establish their correct vectorial superposition. Because of the linearity of Maxwell's equations, the total local field is then obtained as

$$\mathbf{E}_l(\mathbf{r},\omega) = \sum_{i=1}^{2} \begin{bmatrix} A_x{}^{(i)}(\mathbf{r},\omega) \\ A_y{}^{(i)}(\mathbf{r},\omega) \\ A_z{}^{(i)}(\mathbf{r},\omega) \end{bmatrix} [I^{(i)}(\omega)]^{1/2} \exp[i\Phi^{(i)}(\omega)], \tag{1}$$

with spectral intensities $I^{(i)}(\omega)$ and phases $\Phi^{(i)}(\omega)$ of the two polarization-shaped input field components. The local field in the time domain $\mathbf{E}_l(\mathbf{r},t)$ is obtained by separately Fourier transforming each vector component of $\mathbf{E}_l(\mathbf{r},\omega)$.

As an example, we use the near-field geometry shown in Fig. 1 and sideways plane-wave illumination from the $+x$ direction. The 12-fs input laser pulse (Fig. 2) has a Gaussian spectrum. A parabolic spectral phase with a first-order Taylor coefficient of -15 fs and a second-order coefficient of 100 fs^2 was applied to component 1 (dotted curve), resulting in a -15-fs temporal shift and an up-chirp of this component. Component 2 is not shifted in time, but a second-order coefficient of -100 fs^2 leads to a down-chirp. Together, this leads to time-dependent polarization evolution. In an intuitive representation (Fig. 2, right), time evolves from left to right, and ellipses indicate the momentary polarization states and amplitudes of electric field oscillations.[8,9] The gray shading signifies the momentary oscillation frequency, whereas the shadows represent the amplitude envelopes of components 1 and 2 separately. Although the polarization evolves in a complex fashion, at each instant the light pulse is still transversely polarized with respect to the axis of propagation.

However, the local near field acquires contributions along all three polarization directions (the term "polarization" in the context of nonpropagating near fields simply indicates the vector direction of the electric field). The result is illustrated in Fig. 3 for one sample point $P(\mathbf{r})$, with temporal oscillations shown in Fig. 3(a). Component E_y (dashed curve) is parallel to $E^{(2)}$ of the illuminating pulse. Therefore E_y retains some of the far-field characteristics, i.e., the pulse is centered around time zero. Component E_z (dotted curve) is parallel to $E^{(1)}$ and is therefore to some extent translated by -15 fs in time. Of course, the near-field modes introduce further pulse structure and nontrivial mixing between all components. Apart from this, E_x (solid curve) has a significant amplitude of approximately one fourth of the components E_y and E_z, although it is not present in the far field. The phase relations among $E_x(t)$, $E_y(t)$, and $E_z(t)$ vary as functions of time, and these variations in turn

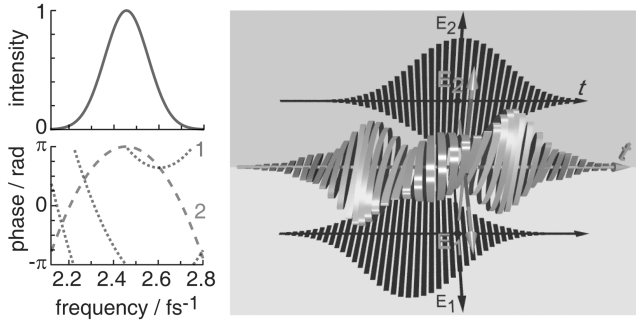

Fig. 2. Far-field evolution. The 12-fs input laser pulse has a Gaussian spectrum, but simple polynomial phase structures (left) lead to a time dependence of the transverse polarization (right), shown over a time interval of 100 fs. More-complex evolutions are possible as well.

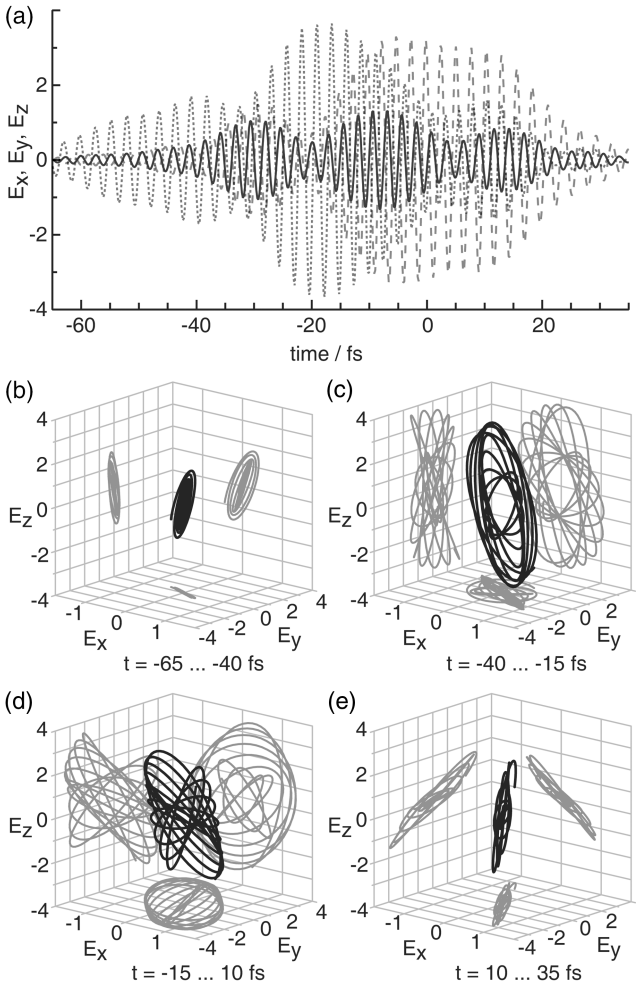

Fig. 3. Near-field evolution. The electric field at $\mathbf{r}/\text{nm} = (-20, 20, 27.5)$ contains three polarization components: (a) the temporal evolution of E_x (solid curve), E_y (dashed curve), and E_z (dotted curve). Parametric plots (b)–(e) show how the electric field vector oscillates in a complex yet controllable fashion in 3D space (black curves) as well as in planar projections (gray curves).

depend on the pulse shaper settings. For example, in Fig. 3(a) at $t = 15$ fs the solid curve is out of phase with the mutually in-phase dotted and dashed curves, whereas at $t = -15$ fs the dashed and dotted curves oscillate with opposite phase and the solid curve is shifted by approximately 90°.

Such behavior results in a complex 3D vectorial time evolution of the electric field. In the beginning the light field is mainly linearly polarized [Fig. 3(b)] but then changes ellipticity as well as orientation in 3D space as time progresses [Figs. 3(c)–3(d)]. Finally it oscillates again mainly linearly polarized but in a different direction [Fig. 3(e)]. The time-dependent polarization state of the incoming laser pulse influences both the individual amplitudes and the phases of different near-field modes, which provides a means of controlling the temporal and spatial evolution of the near-field distribution. The control mechanism is based on linear superposition according to Eq. (1). Constructive versus destructive interference can be used to enhance or suppress near-field modes. The two interfering terms are provided by the two external polarization components, whereas with linearly polarized fields this superposition scheme is not available.

A general assessment of the possible degree of control is difficult, but a discussion of the rate of polarization variation for transversely polarization-shaped fields[9] can in principle be transferred to the near-field scheme. Full controllability requires three independently phase-and-amplitude-shaped beams from different spatial directions and nontrivial mutual phase stabilization, whereas our scheme employs only one external source and therefore requires no phase stabilization. The accessible field distributions are limited by the chosen geometry, the material response, and the spectrum and incidence angle of the illumination. However, the choice of a suitable geometry and the large number of LCD settings (approximately 10^{600}) allows us to create electric fields sufficiently similar to the desired target, as can be deduced from the many successful applications of phase-only linear pulse shaping.[2,3] Similarly, it is possible here to use a learning algorithm for optimal generation of specific electric field profiles and different optimization objectives.[14]

Many potential applications exist for this 3D pulse-shaping technique. For example, selective production of chemical enantiomers (chirality control) could make use of shaped electric fields with three polarization components.[15] Another area involves near-field techniques. For instance, near-field fluorescence microscopy based on two-photon excitation was demonstrated with unshaped femtosecond laser pulses,[11] and near-field interference spectroscopy was also developed.[16] Here the perspective of pulse shaping could increase contrast ratios or combine chemical quantum control methods and microscopy. The effect of linear chirp on local field enhancement has also been reported[17] but without taking into account polarization shaping.

The whole area of nanophotonics could benefit, for example, the optimized action of nanophotonic switching devices.[18] Apart from new perspectives in all these cases, 3D shaping offers the possibility of extending the methods of adaptive quantum control[2,3] to their most general form: With light–matter interaction determined by $\boldsymbol{\mu} \cdot \mathbf{E}(t)$ and the ability to control $\mathbf{E}(t)$ vectorially it is possible to follow and exploit the 3D time evolution of quantum wave functions as probed by the dipole operator $\boldsymbol{\mu}$. Furthermore, spatial field dependency $\mathbf{E}(\mathbf{r}, t)$ can lead to new effects because $\boldsymbol{\mu} \cdot \mathbf{E}(\mathbf{r}, t)$ can vary within the length scale of extended wave functions.

In summary, we have described a novel pulse-shaping technique that allows, for the first time to our knowledge, the shaping of all three mutually orthogonal polarization components of femtosecond light pulses. As a result, the electric near-field vector oscillates within 3D space in a complex fashion. Especially in connection with learning algorithms, we expect many applications because light–matter interaction can be controlled on a fundamental level.

T. Brixner and W. Pfeiffer thank G. Gerber for his support. T. Brixner thanks the Deutsche Forschungsgemeinschaft and G. Fleming for an Emmy–Noether Fellowship at the University of California, Berkeley. F. J. Garcia de Abajo acknowledges support from the Spanish Ministerio de Ciencia y Tecnología (contract MAT2001-0946). W. Pfeiffer's e-mail address is pfeiffer@physik.uni-wuerzburg.de.

References

1. A. M. Weiner, Rev. Sci. Instrum. **71,** 1929 (2000).
2. S. A. Rice and M. Zhao, *Optical Control of Molecular Dynamics* (Wiley, New York, 2000).
3. T. Brixner and G. Gerber, ChemPhysChem **4,** 418 (2003).
4. A. M. Weiner, D. E. Leaird, J. S. Patel, and J. R. Wullert II, Opt. Lett. **15,** 326 (1990).
5. M. M. Wefers and K. A. Nelson, Opt. Lett. **20,** 1047 (1995).
6. J. C. Vaughan, T. Feurer, and K. A. Nelson, Opt. Lett. **28,** 2408 (2003).
7. T. Brixner and G. Gerber, Opt. Lett. **26,** 557 (2001).
8. T. Brixner, G. Krampert, P. Niklaus, and G. Gerber, Appl. Phys. B **74,** S133 (2002).
9. T. Brixner, Appl. Phys. B **76,** 531 (2003).
10. D. Oron, N. Dudovich, and Y. Silberberg, Phys. Rev. Lett. **90,** 213902 (2003).
11. E. J. Sánchez, L. Novotny, and X. S. Xie, Phys. Rev. Lett. **82,** 4014 (1999).
12. F. J. García de Abajo and A. Howie, Phys. Rev. Lett. **80,** 5180 (1998).
13. F. J. García de Abajo and A. Howie, Phys. Rev. B **65,** 115418 (2002).
14. T. Brixner, J. Schneider, W. Pfeiffer, and F. J. García de Abajo, in *Ultrafast Phenomena XIV*, T. Kobayashi, T. Okada, T. Kobayashi, K. A. Nelson, and S. De Silvestri, eds. (Springer-Verlag, Berlin, to be published).
15. K. Hoki, L. González, and Y. Fujimura, J. Chem. Phys. **116,** 8799 (2002).
16. A. A. Mikhailovsky, M. A. Petruska, M. I. Stockman, and V. I. Klimov, Opt. Lett. **28,** 1686 (2003).
17. M. I. Stockman, S. V. Faleev, and D. J. Bergman, Phys. Rev. Lett. **88,** 067402 (2002).
18. T. Kawazoe, K. Kobayashi, S. Sangu, and M. Ohtsu, Appl. Phys. Lett. **82,** 2957 (2003).